ELSEVIER

Chemical Engineering Journal 84 (2001) 295–308

Chemical Engineering Journal

www.elsevier.com/locate/cej

A new diffusion and flow theory for activated carbon from low pressure to capillary condensation range

H.D. Do, D.D. Do*

Department of Chemical Engineering, University of Queensland, St. Lucia, Qld 4072, Australia

Received 24 October 2000; accepted 8 November 2000

Abstract

In this paper, we develop a theory for diffusion and flow of pure sub-critical adsorbates in microporous activated carbon over a wide range of pressure, ranging from very low to high pressure, where capillary condensation is occurring. This theory does not require any fitting parameter. The only information needed for the prediction is the complete pore size distribution of activated carbon. The various interesting behaviors of permeability versus loading are observed such as the maximum permeability at high loading (occurred at about 0.8–0.9 relative pressure). The theory is tested with diffusion and flow of benzene through a commercial activated carbon, and the agreement is found to be very good in the light that there is no fitting parameter in the model. © 2001 Elsevier Science B.V. All rights reserved.

Keywords: Diffusion; Condensation; Permeability

1. Introduction

This paper addresses a theory about the diffusion and flow of adsorbing vapors through activated carbon. Work in the literature have assumed that the transport mechanism is that composing of pore volume diffusion (Knudsen) diffusion, viscous flow and surface diffusion. The first two processes are relatively well studied and understood, while the process of surface diffusion is not fully understood, despite many work have discussed and reviewed this aspect. Among these work, may different models have been proposed to describe the surface transport of adsorbed molecules. Some are based on the thermodynamics argument such as the Darken model and its many variants, some of which account for the surface heterogeneity [8–11,21,25,26,32,46], while a few have assumed hydrodynamics model [19] and some structural models for activated carbon [13]. The reasons for our lack of full understanding of the surface diffusion are as follows:

1. The activated carbon surface is very complex to be idealized as a "perfect" surface.
2. Adsorbed molecules are not perfectly located on a surface, where the usual concept of hopping could be applicable.

Activated carbon is known for its strong heterogeneity, and one factor that contributes to this is the pore size distribution and pore topology. For adsorption equilibrium at relative low pressure, only the distribution of the micropores is sufficient to study the adsorptive capacity as adsorption on mesopore and macropore's surfaces is not significant. Distribution of the mesopores and larger pores is only needed when one is interested in the adsorption over the region where capillary condensation occurs at high pressure. For adsorption kinetics, however, the complete pore size distribution is necessary for the full description of mass transfer from very low pressure to high pressure where capillary condensation is occurring. Pore volume diffusion and viscous flow are dominating in macropores and mesopores, while the surface diffusion is dominating in the micropores and mesopores. We will discuss more about the nature of surface diffusion in activated carbon as the term surface diffusion is somewhat misleading in the context of activated carbon. This is very understandable as surface is not well defined in activated carbon and the usual concept of sub-monolayer surface coverage for the applicability of the surface diffusion does not apply to activated carbon as we shall show later.

The diffusive nature of mass transfer is expected to dominate at very low pressure, while the hydrodynamics will control when the capillary condensation has occurred at high pressures. In between one would expect the combination of diffusion and hydrodynamic flow will contribute to the overall mass transfer through the porous medium. The complication of all this is the complex structure of the porous medium, as well as the different behaviors of different flow and diffusion mechanisms. The topology is important in controlling of the flow, especially in the region of condensation where partial condensation is some pore

* Corresponding author. Tel.: +61-7-3365-4154; fax: +61-7-3365-2789.
E-mail address: duongd@cheque.uq.edu.au (D.D. Do).

1385-8947/01/$ – see front matter
PII: S1385-8947(00)00383-1

Nomenclature

A	pre-exponential coefficient of Eq. (2)
C	coefficient of the BET equation
C_p	coefficient of the *n*-BET equation for adsorption in pores
C_s	coefficient of the *n*-BET equation for adsorption onto a flat surface
d	characteristic pore dimension
n	number of adsorbate layers
N	Avogadro's number
P	system pressure
P_0	relative pressure
Q	heat of adsorption
Q_p	heat of adsorption into a pore
Q_s	heat of adsorption onto a flat surface
r	pore radius
r_k	pore radius from the Kelvin equation
r_{max}	upper limit of the mesopore range
R	universal gas constant
S	surface area
t	statistical thickness of the adsorbate film layer
t_m	thickness of a single layer of the adsorbate
T	temperature
v_M	liquid molar volume
V	pore volume
V_m	monolayer volume

Greek symbols

γ	liquid surface tension
ε_l	reduced heat of liquefaction
$\Delta\varepsilon_l$	the excess of the reduced liquefaction heat
ε_1	reduced energy of adsorption
ε_{12}	nitrogen–carbon interaction energy
θ	liquid–solid contact angle
σ_{12}	collision diameter of the nitrogen–carbon interaction

may block the flow. This aspect has been addressed by many authors, notably Carman and Raal [5–7], Flood et al. [16–18], Debye and Cleland [12], Eberly and Vohsberg [14], Hwang and co-workers [28,39], Okazaki and co-workers [33,40], Haynes and Miller [20], Tsujikawa et al. [41], Abeles et al. [2], Uhlhorn et al. [44], Yang and co-workers [9,38], Petropoulos [36], Petropoulos and Papadopoulos [34,35], van der Zanden and co-workers [1,45] and Kanellopoulos and co-workers [24,27,42,43]. Many of these work deal with only mesoporous solids, and none of them consider the enhancement of adsorption and its consequence in the diffusion and flow from very low pressure to high pressure where capillary condensation is occurring. What we shall address in this paper is the flow of sub-critical vapors for microporous activated carbon as this is important in the area of environmental control of removing solvents from air.

2. Theory

In the development of this theory, we shall derive the basic equations applicable for a single pore, and then obtain the overall equation in terms of the assumed known pore size distribution and assumed random pore structure. The pore geometry is considered as slit shaped. This choice is chosen purely because real pores have arbitrary shape and size, and they do not strictly conform to slit or cylinder. Only in well ordered structures such as zeolite and MCM-41 like solids pore shapes are clearly defined. Another reason for choosing slit shape pore is because micropores in activated carbon are more or less slit-shaped, and it is convenient from the modeling point of view is to retain that shape for all pores.

Adsorption of sub-critical fluids in pores will occur in stages, and different mechanisms occur when pressure is increased from vacuum to vapor pressure. The different mechanisms for diffusion and flow in a pore of half width r are shown in Fig. 1. When the pressure is very low, adsorption mainly occurs on the surface. Here, we have what is called the sub-monolayer adsorption, and the movement of these adsorbed molecules is that of diffusive nature, the process of which can be regarded as hopping of adsorbed molecules from a low potential energy point to another low potential energy point, crossing an energy barrier. The process is called activated surface diffusion. When the pressure is increased to some pressure P_m (usually about one-tenth of the vapor pressure) a monolayer of adsorbate molecules is formed on the surface, and the process of movement is still that of surface diffusion. When pressure is increased beyond P_m, multilayers of adsorbate are formed on top of the first layer. The movement of the first layer is still that of surface diffusion, but the rate is diminishing due to the decrease in the surface concentration of the first layer. The movement of liquid film above the first layer is that of hydrodynamic in nature. These two processes will occur in parallel, and obviously the contribution from the surface diffusion of the first layer will become less significant compared to the hydrodynamic flow of higher layers when pressure is increased. When the pressure is approaching a threshold pressure P^*, the capillary condensation will occur and liquid adsorbate will fill completely the whole volume of the pore. Now we have the capillary condensate flow.

Before describing the fluxes of these processes, we need to present the definitions of various concentration and the driving force for diffusion and flow.

2.1. Equilibrium between the two phases

This section will consider the derivation of the adsorbed phase pressure as a function of the gas phase. This is achievable by assuming the two phases are in equilibrium with each other, then we have the following equality of chemical potentials [3]:

$$\mu_A = \mu_G \text{ (J/mol)} \tag{1a}$$

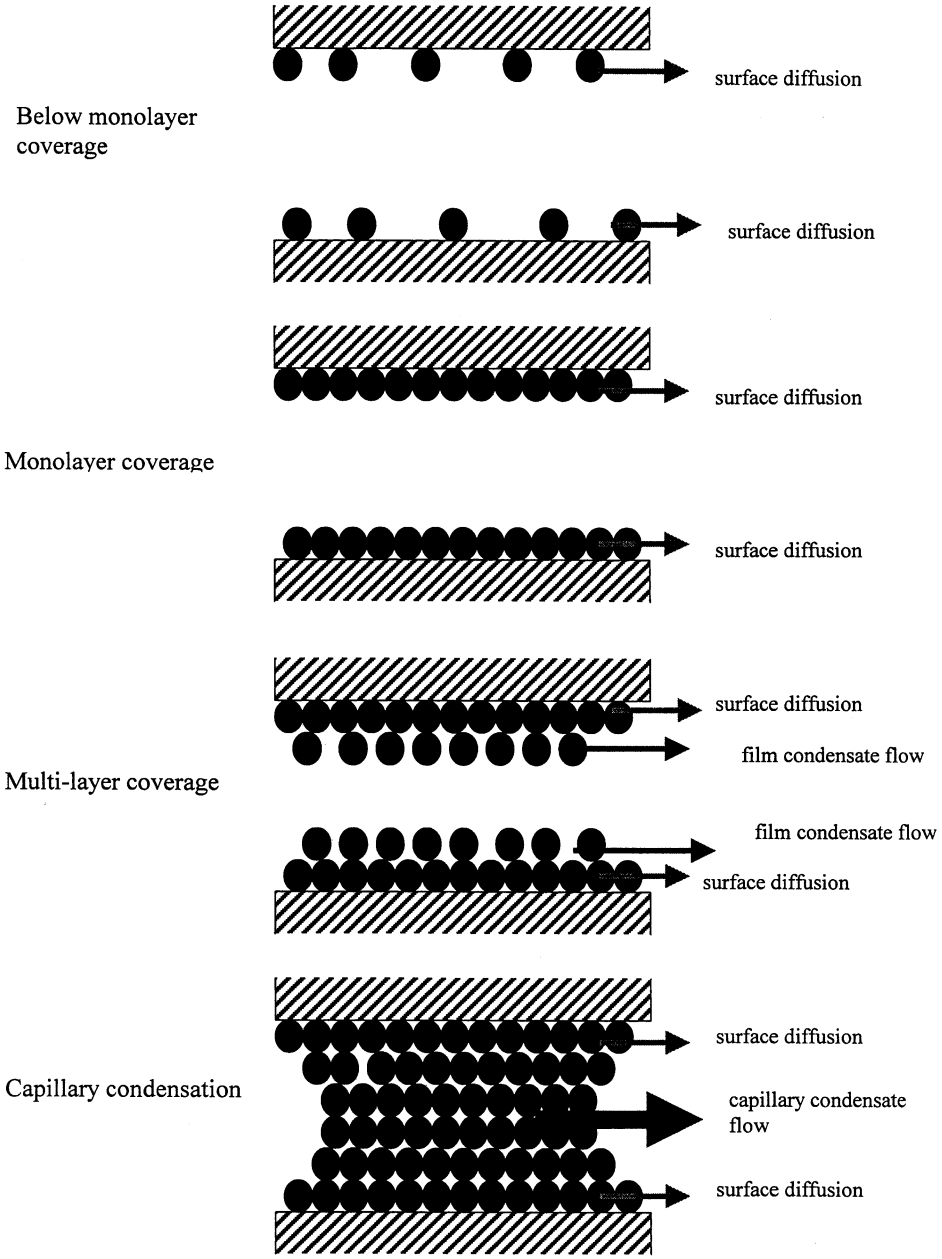

Fig. 1. Different regimes of diffusion and flow of adsorbate molecules through a pore.

or the differential changes in chemical potentials are the same

$$\mathrm{d}\mu_{\mathrm{A}} = \mathrm{d}\mu_{\mathrm{G}} \tag{1b}$$

Here the subscripts A and G are for adsorbed and gas phases, respectively.

Under isothermal conditions, the change of the chemical potential is simply the molar volume of that phase times the change in the pressure of that phase, that is

$$\bar{V}_{\mathrm{A}}\,\mathrm{d}P_{\mathrm{A}} = \bar{V}_{\mathrm{G}}\,\mathrm{d}P \tag{2}$$

Therefore under equilibrium the change in pressure in the adsorbed phase is related to the change in pressure in the gas phase as written below

$$\frac{\mathrm{d}P_{\mathrm{A}}}{\mathrm{d}z} = \frac{\overline{V}_{\mathrm{G}}}{\overline{V}_{\mathrm{A}}}\frac{\mathrm{d}P}{\mathrm{d}z} \tag{3}$$

Assuming the ideal gas behavior, the gas phase molar volume is related to the pressure as $\overline{V}_{\mathrm{G}} = RT/P$, and the adsorbed phase behaves like a liquid phase, that is $\overline{V}_{\mathrm{A}}$ is the liquid molar volume v_{M} (m^3/mol), then the change in pressure in the adsorbed phase is

$$\frac{\mathrm{d}P_{\mathrm{A}}}{\mathrm{d}z} = \frac{RT}{v_{\mathrm{M}}P}\frac{\mathrm{d}P}{\mathrm{d}z} = \frac{RT}{v_{\mathrm{M}}}\frac{\mathrm{d}\ln P}{\mathrm{d}z} \tag{4}$$

This change in liquid phase pressure is much larger than the change in the gas phase because the liquid molar volume is much smaller than the gaseous molar volume. To show an example, we take an example of *n*-butane at 273 K. At this temperature the vapor pressure is 1.04×10^5 Pa, the liquid density is 600 kg/m^3. For a mean pressure of $0.4P_0$, the change in liquid pressure is about 560 times greater than the change in the gas phase pressure, showing that the driving force in the liquid phase is far greater than that in the gas phase. One must also note that despite the liquid driving force is greater, the resistance to flow is also greater, for example the viscosity in the gas phase is of the order of 1×10^{-5} Pa s and that for liquid phase is 1×10^{-3} Pa s.

2.2. Diffusion flux of the first adsorbed layer

Surface diffusion, by its strict definition, represents the mobility of adsorbed molecules below monolayer coverage. The surface diffusion flux is driven by a chemical potential gradient multiplied by the surface concentration per unit surface area. Under local equilibrium between the two phases, the mass transfer of the adsorbed layer (below the monolayer coverage) is assumed to be driven by the gradient of the chemical potential, that is,

$$J_s = -LC_s \frac{\partial \mu}{\partial z} \text{ (mol/m s)} \tag{5}$$

where L is the mobility coefficient. The surface flux is defined as mole transported per unit time and per unit perimeter across which the mass is transferred, and the surface concentration is in mole per unit surface area. With the definition of the corrected surface diffusivity $D_s^0 = \text{LRT}$, the surface diffusion flux equation is

$$J_s = -D_s^0 \frac{C_s}{P} \frac{\partial P}{\partial z} \text{ (mol/m s)} \tag{6}$$

in which we have taken $\mu = \mu_0 + RT \ln P$. The corrected diffusivity may depend on concentration, due to a variation in the average mobility with concentration, with disorder, with energy barrier for migration [23]. In the absence of this information, we will consider it as concentration independence. Knowing the flux equation, we can obtain the velocity (flux per unit concentration) of the adsorbed molecule as

$$v_s = -D_s^0 \frac{1}{P} \frac{\partial P}{\partial z} \text{ (m/s)} \tag{7}$$

To derive the mass transfer, we need to introduce a new parameter to describe the system. This parameter is the density function for the cross-sectional area. We denote it $g(r)$ with $g(r)\,\mathrm{d}r$ being the differential cross-sectional area of pores having half width between r and $r + \mathrm{d}r$. If we assume a slit geometry for pores (applicable for small pores in activated carbon), then the total periphery for pores having half width in the range of r and $r + \mathrm{d}r$ is given by

$$\frac{g(r)\,\mathrm{d}r}{r} \text{ (m)} \tag{8}$$

Therefore, the differential rate of mass transfer contributed by the surface diffusion in pores having half width between r and $r + \mathrm{d}r$ is the product of the periphery and the surface diffusion flux, that is

$$\mathrm{d}M_s = -\frac{g(r)\,\mathrm{d}r}{r} \frac{D_s^0 C_s}{P} \frac{\partial P}{\partial z} \text{ (mol/s)} \tag{9}$$

We have derived the rate of mass transfer contributed by the surface diffusion. We now consider next the derivation of the flux in the case where there is liquid film (multiple layers of adsorbate molecules) on the surface. The flux in this case will be contributed by the liquid condensate film with surface diffusion (slip) at the surface.

2.3. The velocity and flux of the condensate film

We now study the flow of condensate film on a surface by considering a pore of half width r measuring from the center of the pore to the surface of the pore wall atoms. This is the physical pore half width. Let "t" be the statistical thickness of the adsorbed film on the solid surface. If we assume that the film behaves as liquid, the force balance over a thin element of the film will give the following equation in terms of the shear stress:

$$\frac{\mathrm{d}}{\mathrm{d}x}(x^s \tau_{xz}) = -\frac{\partial P_L}{\partial z} x^s \tag{10}$$

where z is the distance along the pore, s the shape factor, being 0 for slit shape and 1 for cylinder. The liquid pressure gradient is $\Delta P_L / L$. At the liquid–gas interface, we shall assume that the shear is negligible, that is,

$$x = a, \qquad \tau_{xz} = 0 \tag{11a}$$

where $a = r - t$. At the liquid–solid interface, there will be slip along the surface and this slip is basically due to the mobility of the adsorbed molecules adjacent to the surface (Eq. (7)), that is,

$$x = r, \qquad v_z = -D_s^0 \frac{\partial \ln P}{\partial z} \tag{11b}$$

If we assume that the liquid film behaves like a Newtonian fluid (that is $\tau_{xz} = -\mu_L\,\mathrm{d}v_z/\mathrm{d}x$), the force balance of Eq. (10) can be written in terms of the axial velocity v_z. Solving this resulting equation subject to the boundary conditions (Eqs. (11a) and (11b)), we derive the following velocity distribution across the film (assuming that the viscosity does not vary across the film):

$$v_z(x) = -\left\{ \frac{r^2}{2\mu_L} \left[1 - \left(\frac{x}{r} \right)^2 \right] \frac{\partial P_L}{\partial z} - \frac{r(r-t)}{\mu_L} \times \left[1 - \left(\frac{x}{r} \right) \right] \frac{\partial P_L}{\partial z} + D_s^0 \frac{\partial \ln P}{\partial z} \right\} \tag{12}$$

from which we can calculate the mean velocity as follows:

$$\langle v_z \rangle = -\left(\frac{t^2}{3\mu} \frac{\partial P_L}{\partial z} + D_s^0 \frac{\partial \ln P}{\partial z} \right) \tag{13}$$

The last term is the slip velocity due to the motion of the first layer. When the pore is completely filled with liquid, that is at pressure greater than the capillary condensation pressure the mean velocity is

$$\langle v_z \rangle = -\left(\frac{r^2}{3\mu_L} \frac{\partial P_L}{\partial z} + D_s^0 \frac{\partial \ln P}{\partial z} \right) \text{ (m/s)} \tag{14}$$

where the statistical thickness of the film has been replaced by the pore half width.

Knowing the film velocity as given in Eq. (13), the molar flow rate of the liquid film per unit cross-sectional area of the liquid film is

$$J = \left(\frac{1}{v_M} \right) \langle v_z \rangle \text{ (mol/m}^2\text{ s)} \tag{15}$$

where v_M is the liquid molar volume. For pores having radii between r and $r + dr$, the fraction of the pore cross-section occupied by the liquid condensate film is $(t/r)g(r)\,dr$. Thus the rate of mass transfer by the liquid condensate is

$$dM_L = -\left(\frac{t}{r} \right) \left(\frac{g(r)\,dr}{v_M} \right) \times \left(\frac{t^2}{3\mu_L} \frac{\partial P_L}{\partial z} + D_s^0 \frac{\partial \ln P}{\partial z} \right) \text{ (mol/s)} \tag{16}$$

Written in terms of the pressure gradient in the gaseous phase (Eq. (4)), the above equation will become

$$dM_L = -\left(\frac{g(r)\,dr}{r} \right) \left(\frac{t^3}{3\mu_L} \frac{RT}{v_M^2} + D_s^0 \frac{t}{v_M} \right) \frac{\partial \ln P}{\partial z} \text{ (mol/s)} \tag{17}$$

We see that the term t/v_M is the surface concentration if t is statistically less than the thickness of one monolayer. Comparing this equation with that for surface diffusion (Eq. (9)), we see that the mass transfer rate of the adsorbed phase can be combined in one form

$$dM_L = -\left(\frac{g(r)\,dr}{r} \right) \times \left(\frac{H(t-\sigma)(t-\sigma)^3}{3\mu_L} \frac{RT}{v_M^2} + D_s^0 C_s \right) \times \frac{\partial \ln P}{\partial z} \text{ (mol/s)} \tag{18}$$

where the surface concentration C_s is defined as

$$C_s = \begin{cases} \dfrac{t}{v_M} & \text{for } t < \sigma \\ \dfrac{\sigma}{v_M} & \text{for } t > \sigma \end{cases} \tag{19}$$

Here σ is the thickness of one monolayer. In Eq. (18), $H(\cdot)$ is the Heaviside step function, where we assume that only the molecules in the second and higher layers contribute to the flow of viscous nature. The first layer flows according to the diffusive action. The above equation reduces to the surface diffusion equation (Eq. (9)) when the thickness is less than the monolayer thickness.

2.4. The gaseous flux

We have derived the mass transfer rate, contributed by the liquid condensate film. Because of the reduction in the cross sectional area due to the presence of condensate film, the mass transfer in the gas phase due to Knudsen diffusion and viscous flow processes is given by

$$dM_G = -\left[\frac{(r-t)g(r)\,dr}{r} \right] \times \left[\frac{D_K(r-t)}{RT} + \frac{B_0(r-t)P}{\mu_G RT} \right] \frac{\partial P}{\partial z} \tag{20}$$

where μ_G is gas phase viscosity, D_K the Knudsen diffusivity, and B_0 the viscous flow parameter for gaseous flow, and they are given by for slit geometry [31]:

$$D_K(r) = \frac{r}{2}\sqrt{\frac{8RT}{\pi M}}, \qquad B_0 = \frac{r^2}{3} \tag{21}$$

The first factor in the RHS of Eq. (20) is the fraction of area that contains only free molecules in pores having half width between r and $r + dr$. In principle, this equation remains valid when the film thickness is less than the half width, that is $t < r$. But in fact, due to the pore filling or capillary condensation, the gaseous mass transfer will be zero when the effective pore half width is less than the critical half width, dictated by the capillary condensation equation. This capillary condensation will be addressed next, together with equations for the calculation of the film thickness.

2.5. Film thickness

We have developed some basic ingredient equations for the mass transfer rate contributed by the liquid condensate film and the gas phase when the condensate film thickness is known. Now we will derive equations for the film thickness as a function of pressure, and here we shall allow for the enhancement on the film thickness due to the enhanced interaction between pore surfaces and the adsorbate molecules.

The theory is developed based on the premise that the knowledge about the adsorption on a flat surface can be extended to describe the adsorption occurring in a pore. This approach assumes that the surface chemistry of the flat surface and the surface of the pore walls are similar so that the pore dimension is the only factor that makes adsorption in the pore different from that occurring on a flat surface. We now review basic equations for a flat surface and then propose proper equations applicable for pores of finite dimension.

2.5.1. Single flat surface

Adsorption on a flat surface by a sub-critical fluid gives rise to layering of molecules on the surface, and if the relative pressure is about 0.1 or greater, multilayers of adsorbate molecules will be formed. This has been very well described by the classical BET equation as given below [4]

$$V = V_{\mathrm{m}}\left[\frac{C_{\mathrm{BET}}P}{(P_0 - P)[1 + (C_{\mathrm{BET}} - 1)(P/P_0)]}\right] \ (\mathrm{m}^3/\mathrm{kg}) \tag{22}$$

or in terms of the statistical adsorbed film thickness:

$$t = \sigma\left[\frac{C_{\mathrm{BET}}P}{(P_0 - P)[1 + (C_{\mathrm{BET}} - 1)(P/P_0)]}\right] \ (\mathrm{m}) \tag{23}$$

where σ is the thickness of a monolayer coverage. The coefficient C_{BET} in the above equation is a measure of the adsorptive strength and is given by

$$C_{\mathrm{BET}} = A\exp\left(\frac{Q}{RT} - \frac{\lambda}{RT}\right) \tag{24}$$

Here λ is the heat of liquefaction (J/mol), and Q the energy of interaction between the first layer of adsorbate with the surface. For an energetic homogeneous flat surface this energy of interaction is a constant. However, when we deal with pores having dimension comparable to that of adsorbate molecule, which is what we are doing here, this energy is a function of pore size because of the overlapping of the potential fields exerted by the two sides of the pore [15]. This energy of interaction is greater when the pore size gets smaller, but when the half width (defined as from the pore center to the center of surface atoms) is about equal to the collision diameter the interaction energy will be decreased owing to the strong repulsive forces caused by the greater proximity of the two walls of the pore. When C_{BET} is greater in pores, the amount adsorbed will be greater and hence the liquid film will be thicker compared to the single flat surface.

2.5.2. Adsorption in a confined space of slit geometry

Adsorption in a confined space is in a way similar to that on a flat surface. The differences are that the number of layers allowable in the pore (n) is finite, and the constant C_{BET} is enhanced due to the overlapping of the potential fields exerted by the two opposite walls of the slit pore. Although, strictly speaking we should allow only n layers in the adsorption BET-type isotherm equation, we can still use the classical BET equation (Eq. (23)) for the calculation of the film thickness. This does not cause any significant errors as the pore filling or capillary condensation mechanism will take over well before the multilayering occurs to n layers. Not only the C_{BET} constant is enhanced in pores, the gaseous pressure in pore is also enhanced, again due to the overlapping of the potential field. It can be calculated as follows:

$$P_{\mathrm{pore}} = P\exp\left(-\frac{\alpha E_0}{RT}\right) \tag{25}$$

where E_0 is the potential energy when the adsorbate molecule is put in the center of the pore. Here, we introduce the factor α to account for the fact that not all free molecules in the pore are subject to the same potential E_0.

The coefficient C_{BET} is regarded as constant for a flat surface, but for pores of finite dimension, this constant C_{BET} varies with the energy of interaction Q. Since Q is a function of the pore half width, the coefficient C_{BET} is also a function of pore size. Assuming the pre-exponent coefficient A does not change with pore size, we write

$$C_{\mathrm{BET,s}} = A\exp\left(\frac{Q_{\mathrm{s}}}{RT} - \frac{\lambda}{RT}\right) \tag{26a}$$

$$C_{\mathrm{BET,p}}(r) = A\exp\left(\frac{Q_{\mathrm{p}}(r)}{RT} - \frac{\lambda}{RT}\right) \tag{26b}$$

the relationship between the constant C_{BET} for a flat surface and that for a pore is

$$C_{\mathrm{BET,p}}(r) = C_{\mathrm{BET,s}}\exp\left(\frac{Q_{\mathrm{p}}(r) - Q_{\mathrm{s}}}{RT}\right) \tag{27}$$

where the subscripts p and s denote for pore and flat surface, respectively. The BET equation (Eq. (22)) and the corresponding film thickness (Eq. (23)) for a pore of half width r can now be calculated using the above value of $C_{\mathrm{BET,p}}(r)$ and the pressure P being replaced by P_{pore}. To calculate the BET constant for a pore, we have to calculate the heat of adsorption in a pore. Heat of adsorption can be calculated as the decrease in the potential energy of the adsorbate when transferred from the bulk gas phase to the adsorbed state. Thus, theoretically the heat of adsorption Q at zero loading can be taken as the depth of the potential energy profile of the first adsorbed molecules. This minimum can be obtained by summing all the pairwise interaction energies of the form of Lennard–Jones 12-6 between the adsorbate molecule and the surface atoms of the two walls. By assuming a configuration for the two surfaces for the carbon wall [29], we can readily determine the minimum potential energy as a function of pore size. The potential enhancement is highest when the pore half width is approximately equal to the collision diameter of the adsorbate and the surface atom. The exact pore half width at which the enhancement is greatest depends on the pore configuration chosen.

2.5.3. Pore filling or capillary condensation process

We have mentioned before that except for pores of very small dimension, the layering of molecules on the two walls will not meet at the center because before this could happen the capillary condensation or pore filling will occur. We shall assume here that the mechanism of pore filling in micropores and that of capillary condensation in mesopores are the same. The difference in these two is the enhancement of the gaseous pore pressure and the enhancement of the film thickness in micropores as discussed in the last section. The pore filling or capillary condensation phenomenon can be

described by the following equation, written below for a slit shaped geometry [22,23]:

$$\frac{r_k(P) - t(P,r) - \sigma_s}{2} = -\frac{\gamma v_M}{RT\ln(P/P_0)} \tag{28}$$

where σ_s is the collision diameter of the surface atom, γ the surface tension (N/m), and v_M the liquid molar volume (m^3/mol). This equation is argued to be applicable for not just mesopores but also micropores as well [30], where we argued that the failure of the Kelvin equation in predicting the diameter of smaller pores rests mostly on the incapability of the estimation of the statistical adsorbed film thickness t. This enhancement in the film thickness has been addressed in the last section. Combining Eqs. (28) and (23), we can determine the threshold pressure as a function of pore half width. In general the larger is the pore, the larger is the condensation pressure. But this is a general rule, as for very small sub-micropores where the repulsive forces are very strong and the condensation pressure would be very high in those pores as well. Most of these pores are usually inaccessible to adsorbate molecules, and the fraction of these pores is usually very small compared to other pores; therefore, these small pores will be ignored from our work.

Solving the pore filling equation, we will get the pore filling pressure as a function of the pore half width, which is typically shown in Fig. 2 for benzene in activated carbon at 303 K. We see that when the pressure is less than P^*, there will be no condensation in any pore. As the pressure is greater than P^*, there will be two solutions for the pore half width. We denote them r_1 and r_2, and pores having radii between r_1 and r_2 will be filled with adsorbate molecules. This threshold pressure P^* is usually very low, usually too low to practically measure.

2.6. The total mass transfer and permeability

We have now derived all the necessary equations for the development of total mass transfer equation. Assuming all the pores are arranged in random, the total mass transfer rate for $P < P^*$ is

$$M = -\left\{\int_0^\infty \left(\frac{g(r)\,dr}{r}\right)\left(D_s^0\frac{C_s}{P}\right) + \left(\frac{r-t}{r}\right)g(r)\,dr \times \left[\frac{D_K(r-t)}{RT} + \frac{B_0(r-t)P}{\mu_G RT}\right]\right\}\frac{\partial P}{\partial z}\ (\text{mol/s}) \tag{29}$$

which is just purely the sum of the surface diffusion and pore Knudsen diffusion and gaseous viscous flow.

When $P > P^*$, pore filling will occur in pores having radii between r_1 and r_2. In such a case, the mass transfer rate will be a summation of three terms. The first term is contributed by pores having radii between 0 and r_1, where layering is occurring, the second term is contributed by pores having radii between r_1 and r_2, where all pores have been filled. Finally, the last term is contributed by pores having radii greater than r_2, where layering is occurring. The equation is

$$\begin{aligned} M =& -\left\{\int_0^{r_1}\left(\frac{g(r)\,dr}{r}\right)\left(\frac{H(t-\sigma)(t-\sigma)^3RT}{3\mu_L v_M^2 P} + D_s^0\frac{C_s}{P}\right)\right. \\ &\left. + \left(\frac{r-t}{r}\right)g(r)\,dr\left[\frac{D_K(r-t)}{RT} + \frac{B_0(r-t)P}{\mu_G RT}\right]\right\} \\ &\times\frac{\partial P}{\partial z} - \left\{\int_{r_1}^{r_2}\left(\frac{g(r)\,dr}{r}\right)\left(\frac{(r-\sigma)^3RT}{3\mu_L v_M^2 P} + D_s^0\frac{C_s}{P}\right)\right\} \\ &\times\frac{\partial P}{\partial z} - \left\{\int_{r_2}^{\infty}\left(\frac{g(r)\,dr}{r}\right)\left(\frac{H(t-\sigma)(t-\sigma)^3RT}{3\mu_L v_M^2 P}\right.\right. \\ &\left.\left. + D_s^0\frac{C_s}{P}\right) + \left(\frac{r-t}{r}\right)g(r)\,dr \right. \\ &\left.\times\left[\frac{D_K(r-t)}{RT} + \frac{B_0(r-t)P}{\mu_G RT}\right]\right\}\frac{\partial P}{\partial z} \end{aligned} \tag{30a}$$

Since the contribution of pores having radii smaller than r_1 is very small, we can neglect its contribution to the total flux because not only adsorbate molecules have difficulty in getting into those pores, the mobility is also expected to be extremely low. Thus, the mass transfer equation can be replaced by

$$\begin{aligned} M =& -\left\{\int_0^{r_2}\left(\frac{g(r)\,dr}{r}\right)\left(\frac{(r-\sigma)^3RT}{3\mu_L v_M^2 P} + D_s^0\frac{C_s}{P}\right)\right\}\frac{\partial P}{\partial z} \\ &-\left\{\int_{r_2}^{\infty}\left(\frac{g(r)\,dr}{r}\right)\left(\frac{H(t-\sigma)(t-\sigma)^3RT}{3\mu_L v_M^2 P} + D_s^0\frac{C_s}{P}\right)\right. \\ &\left. + \left(\frac{r-t}{r}\right)g(r)\,dr \right. \\ &\left.\times\left[\frac{D_K(r-t)}{RT} + \frac{B_0(r-t)P}{\mu_G RT}\right]\right\}\frac{\partial P}{\partial z} \end{aligned} \tag{30b}$$

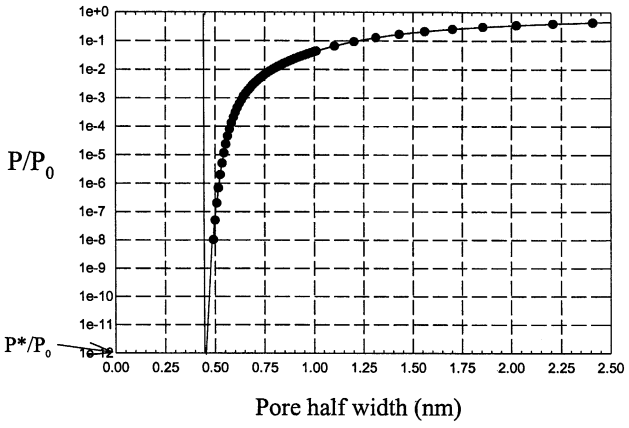

Fig. 2. Pore filling pressure of benzene at 303 K versus pore half width.

where we basically assume that pores having radii less than r_2 will be filled with adsorbate, and those having radii greater than r_2 have layering process occurring in them.

The total permeability is defined as

$$M = -A_p B \frac{\partial P}{\partial z} \tag{31}$$

where A_p is the total cross-sectional area, which is

$$A_p = \frac{1}{\varepsilon}\int_0^\infty g(r)\,dr \tag{32}$$

where ε is the initial total porosity, that is the ratio of all pores volume to the particle volume. Thus, comparing Eqs. (30a), (30b) and (31), we derive the following equation for the total permeability:

$$B = \varepsilon\int_0^\infty \left\{\left(D_s^0\frac{C_s}{P}\right) + (r-t) \times\left[\frac{D_K(r-t)}{RT} + \frac{B_0(r-t)P}{\mu_G RT}\right]\right\} \times\left(\frac{\alpha(r)\,dr}{r}\right)\ (\mathrm{mol/(m\,s\,Pa)}) \tag{33a}$$

for $P < P^*$, and

$$B = \varepsilon\int_0^{r_2}\left(\frac{(r-\sigma)^3 RT}{3\mu_L v_M^2 P} + D_s^0\frac{C_s}{P}\right)\left(\frac{\alpha(r)\,dr}{r}\right) + \varepsilon\int_{r_2}^\infty\left\{\left(\frac{H(t-\sigma)(t-\sigma)^3 RT}{3\mu_L v_M^2 P} + D_s^0\frac{C_s}{P}\right) + (r-t)\left[\frac{D_K(r-t)}{RT} + \frac{B_0(r-t)P}{\mu_G RT}\right]\right\}\left(\frac{\alpha(r)\,dr}{r}\right) \tag{33b}$$

for $P > P^*$. Here $\alpha(r)\,dr$ is the fraction of pore having radii between r and $r + dr$, and is defined as

$$\alpha(r) = \frac{g(r)}{\int_0^\infty g(r)\,dr} \tag{33c}$$

Let us consider the extreme case of very low pressure where the film condensate flow is negligible. For this case the permeability is

$$B = \varepsilon\int_0^\infty\left\{\left(\frac{1}{r}\frac{D_s^0 C_s}{P}\right) + \left[\frac{D_K(r)}{RT} + \frac{B_0(r)P}{\mu_G RT}\right]\right\}\alpha(r)\,dr \quad (\mathrm{mol/(m\,s\,Pa)}) \tag{34a}$$

For activated carbon, this permeability is very difficult to measure as the pressure required for this to occur is very low. Nevertheless, when this is feasible, this permeability will be a constant as the ratio of the surface concentration C_s to P is a constant (true Henry constant) and the viscous flow contribution will be negligible compared to the Knudsen flow at this very low pressure. Thus, the zero loading limit of the permeability is (which should be very small):

$$B = \varepsilon\int_0^\infty\left\{\left(\frac{1}{r}D_s^0 K_s\right) + \left[\frac{D_K(r)}{RT}\right]\right\}\alpha(r)\,dr \quad (\mathrm{mol/(m\,s\,Pa)}) \tag{34b}$$

At very high pressure (P approaching the vapor pressure P_0), the permeability is

$$B = \varepsilon\int_0^\infty\left(\frac{(r-\sigma)^3 RT}{3\mu_L v_M^2 P} + D_s^0\frac{C_{sm}}{P}\right)\left(\frac{\alpha(r)\,dr}{r}\right) \tag{35}$$

We see that when the pressure is approaching the vapor pressure, the permeability decreases with pressure. At the vapor pressure, the limiting permeability is

$$B = \varepsilon\int_0^\infty\left(\frac{(r-\sigma)^3 RT}{3\mu_L v_M^2 P_0} + D_s^0\frac{C_{sm}}{P_0}\right)\left(\frac{\alpha(r)\,dr}{r}\right) \tag{36}$$

The two extremes of the permeability indicate that the permeability is a constant at zero loading (as physically expected), and at very high loading the permeability decreases with loading and approaches a limiting value as given in Eq. (36). Since the permeability at zero loading is very small, the pattern of the permeability versus pressure (or loading) should be such that it is increased with loading, and when the pressure is relatively high, the permeability will decrease as governed by Eq. (35) and reaches a limiting value of Eq. (36).

In terms of the dependence on adsorbate properties, we observe that at zero loading the permeability (Eq. (34b)) is approximately inversely proportional to the square root of the molecular weight, because the Knudsen diffusivity is inversely proportional to the molecular weight and the surface diffusivity are approximately inversely proportional to the molecular weight (experimentally we have found that the surface diffusivity decreases faster than $1/\sqrt{MW}$ [37]). If the surface diffusion is very strong, then the permeability is proportional to the slope of the adsorption isotherm at zero loading. At very high loading, the mass transfer is dominated by the liquid condensate flow and by surface diffusion (Eq. (35)). The first contribution is inversely proportional to the liquid phase viscosity, while the latter is inversely proportional to the molecular weight. Usually at this high loading, the contribution of the liquid condensate is greater than that of the surface diffusion. Thus, the permeability is inversely proportional to the liquid phase viscosity.

To ascertain the behavior of the permeability with loading, we need to consider Eq. (33b). At low pressure, the contribution of the second integral is more important than the first one. We see that the Knudsen diffusion contribution is a constant, the viscous flow increases with pressure (not linearly due to the reduction of the pore volume area), and the liquid condensate term increases very fast with pressure due to the increase of $(t-\sigma)^3$ much faster than P. Thus from the knowledge of low pressure and moderate pressure and high pressure, one would expect the behavior of the permeability versus loading as shown schematically in Fig. 3.

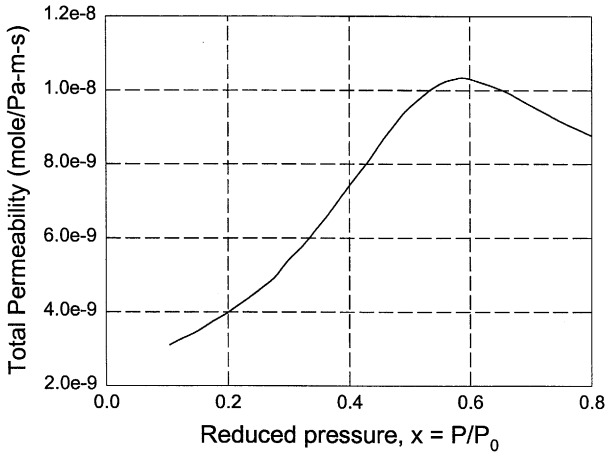

Fig. 3. Typical total permeability versus loading.

2.7. Mass balance equation

Having obtained the permeability in the last section, the mass balance equation for a slab geometry is simply

$$\frac{\partial}{\partial t}(\rho_p C_T) = -\frac{\partial}{\partial z}(J) \tag{37}$$

where C_T is the volumetric total concentration, and J the flux per unit total cross-sectional area and is written explicitly in terms of the pressure gradient and the permeability as

$$J = -B\frac{\partial P}{\partial z} \tag{38}$$

where B is defined in Eqs. (33a)–(33c). The volumetric total concentration is given by

$$C_T = \varepsilon\left(\frac{1}{v_M}\right)\left\{\int_0^{r_1}\left[\frac{t(P,r)}{r}\right]\alpha(r)\,dr + \int_{r_1}^{r_2}\alpha(r)\,dr\int_{r_2}^{\infty}\left[\frac{t(P,r)}{r}\right]\alpha(r)\,dr\right\} \tag{39}$$

Steady state solution of the mass balance equation is simply

$$J_{SS} = -B(P)\frac{\partial P}{\partial z} \equiv \text{constant} \tag{40}$$

Integration of this equation subject to constant boundary conditions:

$$z = 0, \qquad P = P_1 \tag{41a}$$

$$z = L, \qquad P = P_2 \tag{41b}$$

yields the following solution for the steady state flux:

$$J_{SS} = \frac{1}{L}\int_{P_2}^{P_1} B(P)\,dP \tag{42}$$

3. Results and discussion

We have developed a theory for diffusion and flow in the region of capillary condensation. Let us now consider the relative contribution of gas and adsorbed phases toward the total permeability. First, we consider the individual contribution of each pore. For $P < P^*$, that is pressure is below the pore filling pressure in any pore, the ratio of the gas phase permeability to the adsorbed phase permeability is

$$\frac{\text{gas permeability}}{\text{adsorbed phase permeability}} = \frac{(r-t)[(D_K(r-t)/RT) + (B_0(r-t)P/\mu_G RT)]}{D_s^0(C_s/P)} \tag{43a}$$

When $P > P^*$, this ratio is given by

$$\frac{\text{gas permeability}}{\text{adsorbed phase permeability}} = \begin{cases} \dfrac{(r-t)[(D_K(r-t)/RT) + (B_0(r-t)P/\mu_G RT)]}{(H(t-\sigma)(t-\sigma)^3 RT/3\mu_L v_M^2 P) + D_s^0(C_s/P)} & \text{for } r < r_1 \text{ or } r > r_2 \\ 0 & \text{for } r_1 < r < r_2 \end{cases} \tag{43b}$$

Eqs. (43a) and (43b) show the relative contribution of the gas phase to the adsorbed phase, and they are useful to see this relative contribution in each pore. In general, one would expect this ratio is large for large pore, and small for small pore. Since the relative contribution varies from pore to pore, the overall ratio of these contributions can be obtained from Eqs. (33a)–(33c):

$$\frac{\text{overall gas permeability}}{\text{overall adsorbed phase permeability}} = \frac{\int_0^{\infty}\{(r-t)[(D_K(r-t)/RT) + (B_0(r-t)P/\mu_G RT)]\}(\alpha(r)\,dr/r)}{\int_0^{\infty}\{(D_s^0(C_s/P))\}(\alpha(r)\,dr/r)} \tag{44a}$$

for $P < P^*$, and

$$\frac{\text{overall gas permeability}}{\text{overall adsorbed phase permeability}} = \frac{\int_{r_2}^{\infty}\{(r-t)[(D_K(r-t)/RT)+(B_0(r-t)P/\mu_G RT)]\}(\alpha(r)\,dr/r)}{\int_0^{r_2}[((r-\sigma)^3 RT/3\mu_L v_M^2 P)+D_s^0(C_s/P)](\alpha(r)\,dr/r)+\int_{r_2}^{\infty}\{(H(t-\sigma)(t-\sigma)^3 RT/3\mu_L v_M^2 P)+D_s^0(C_s/P)\}(\alpha(r)\,dr/r)} \tag{44b}$$

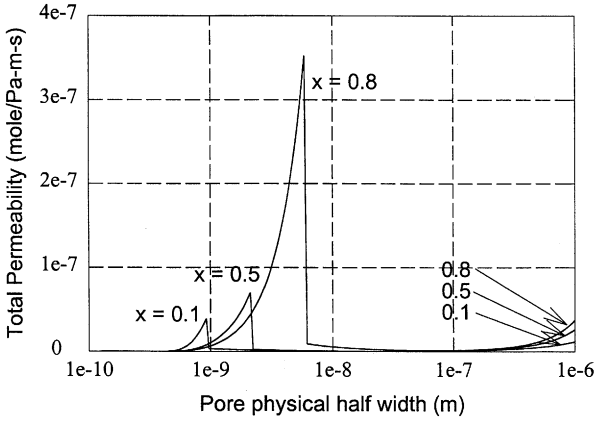

Fig. 4. Permeability as a function of physical pore half width.

The typical behavior of the total permeability versus the reduced pressure as shown in Fig. 3 exhibits an increase with pressure, and then decreases when the pressure has been sufficiently high. Such behavior has been observed by Lee and Hwang, who studied flow of Freon-113 in microporous Vycor glass. It is important that, with the proposed theory presented in this paper, to provide a detailed contribution of various processes on the overall behavior. First, we investigate the dependence of the total permeability versus the physical pore half width (surface to pore center). Fig. 4 shows such behavior for three levels of reduced pressure, $P/P_0 = 0.1, 0.5$ and 0.8. The lowest level represents the situation where adsorption occurs dominantly in small micropores. The middle level is for the situation where adsorption in mesopore starts to become noticeable, and the last level is that where capillary condensation has achieved to a significant degree. First we see that at low loading the permeability is dominated mainly by the micropores, and the permeability is relatively low due to the low conductance of the very small pore. Maximum permeability is achieved at pores having half width of about 10 A. We note that the permeability for mesopores and macropores is practically very small. This is due to the very low loadings in those pores as well as the pressure is low enough to induce any significant Knudsen flow or gaseous viscous flow. These are only significant for pores having size greater than 10 000 A. When the reduced pressure is 0.5, the permeability is now dominated by large micropores and small mesopores. At this level of pressure, all small micropores are completely filled with adsorbate, and the contribution of these small micropores towards the permeability decreases like $1/P$ (see Eq. (35)). Thus the domination is by larger micropores or small mesopores. Again, the larger mesopores and macropores contribute very little to the total permeability. When the reduced pressure is increased to 0.8, the permeability increases significantly from about 1×10^{-7} to 4×10^{-7} mol/(m s Pa). Such a fourfold increase is due to the transport of condensate in the mesopores, which is resulted by the two factors: (a) large density of adsorbate, and (b) high conductance of mesopores compared to micropores. The conductance is defined as the permeability per unit loading.

The general feature we observed in Fig. 4 is the low permeability over the mesopore region, ranging from about 80 to 500 A. This is quite significant to the tailoring of solids to achieve high capacity as well as fast kinetics. The good solids therefore are those that have high proportion of micropores having half width of less than about 50 A and macropores greater than 5000 A. Many good activated carbon, like the one used in our laboratory, have micropores having size less than 30 A and macropores having size greater than 4000 A.

To have a better picture of how permeability changes with pressure, we plot in Fig. 5 the permeability versus pressure for pores of different ranges. For micropores having mean physical pore half width of 5 A, the total permeability decreases with pressure (Fig. 5a). This is due to the fact that over the practical range of pressure, $x > 0.01$, these pores are filled quickly with adsorbate molecules, and the permeability for completely filled pore will decrease with pressure like $1/P$. For micropores having physical pore half width of 20 A (Fig. 5b, curve A), the permeability is approximately constant for reduced pressure less than about 0.2, beyond which it increases very fast with pressure (or loading). This is due to the build-up of adsorbed layers in these pores, which occurs over the region of reduced pressure from 0.2 to about 0.6. Increase in reduced pressure from 0.6 will result in a reduction of the permeability. This is due to the complete filling of these pores, and again the permeability of completely filled pores decreases with P like $1/P$. We also show in Fig. 5b, the permeability of small micropores (5 A) and larger pores (500 and 3000 A) to compare the magnitude of the permeability. This shows the importance of the permeability of the large micropores of 20 A. Fig. 5c shows the permeability of large mesopores (500 A). Here, we see that the Knudsen diffusion permeability dominates the overall permeability until the liquid condensate in these pores has sufficient thickness to contribute to the overall permeability. This occurs at a reduced pressure of about 0.7. For pores of this size, the gaseous viscous flow contribution is very small. When pores are larger (3000 A), Fig. 5d shows that the total permeability is dominated entirely by the Knudsen and gaseous viscous flow. For pores of this size, the contribution from the liquid condensate is negligible and this is due to the very low adsorption in this type of pore.

The effect of variance of the pore size distribution is to spread the permeability curve as shown in Fig. 6a and b for micropores and mesopores, respectively.

We now test the theory with the total permeability of benzene diffusing through an Ajax activated carbon, which has the following properties: BET surface area of 1.2×10^4 m^2/kg, particle density 733 kg/m^3, total porosity 0.71, macropore porosity 0.3 and micropore porosity 0.41. The mean macropore size is 8×10^{-7} m. The pore size distribution of this activated carbon is shown in Fig. 7. This PSD is required in the theory for the calculation of the permeability. A particle (of length 4×10^{-3} m) was mounted between two

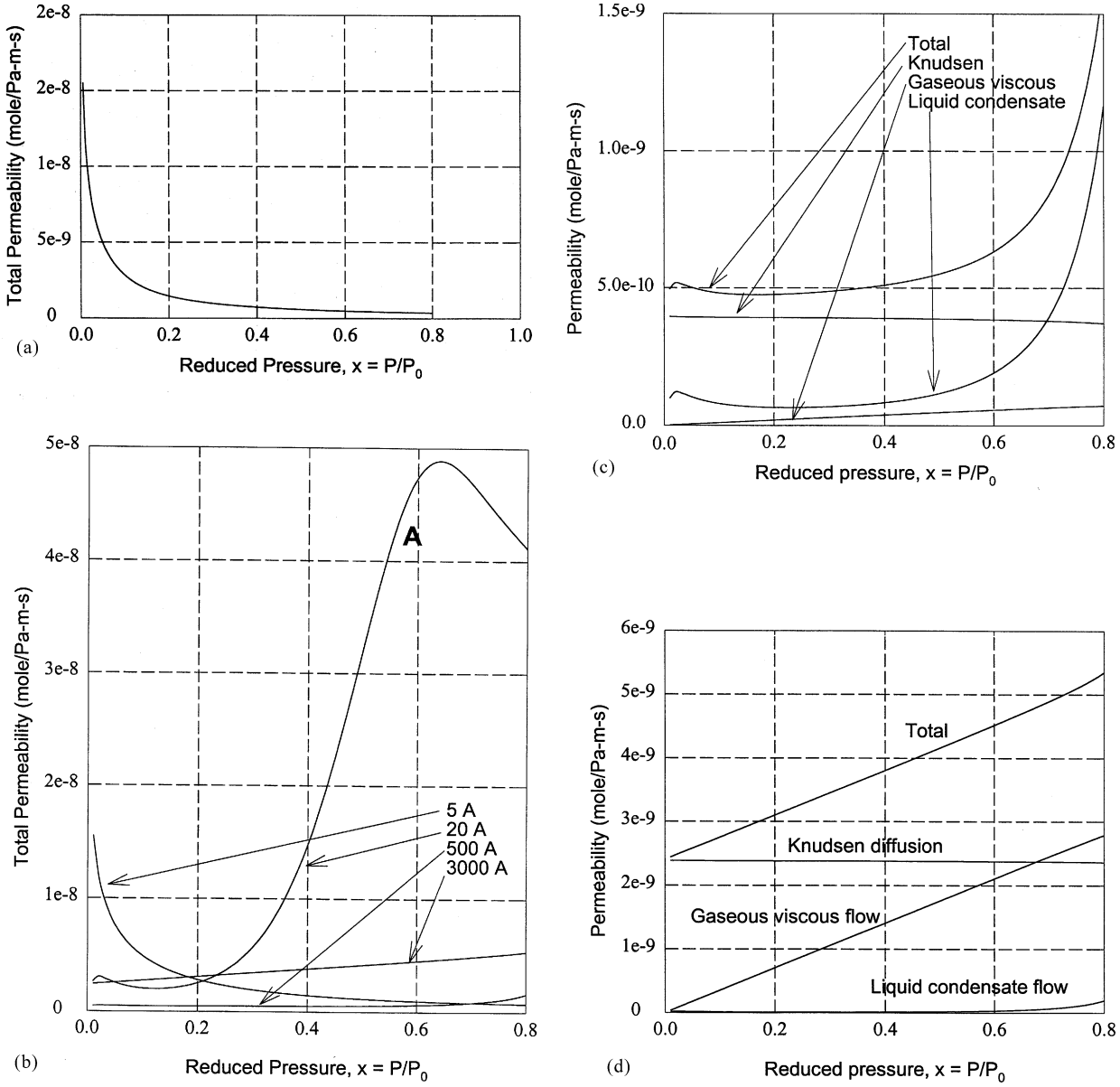

Fig. 5. Permeability as a function of pressure: (a) micropore range ($r = 5\,\text{A}, \sigma = 1.25\,\text{A}$); (b) mesopore range ($r = 20\,\text{A}, \sigma = 5\,\text{A}$); (c) macropore range ($r = 500\,\text{A}, \sigma = 125\,\text{A}$); (d) large macropore range ($r = 3000\,\text{A}, \sigma = 750\,\text{A}$).

reservoirs. The particle–reservoirs assembly was cleaned under ultra-low vacuum (below 10^{-4} Pa) overnight, after which the complete assembly was brought to the adsorption temperature. Once this is achieved, pure vapor was dosed into the system, and sufficient time is allowed for equilibrium to achieve. Let this equilibrium pressure be P^*. The upstream reservoir is then isolated from the particle and downstream reservoir. A small amount of pure gas or vapor was then added into the upstream reservoir to increase the pressure by $\Delta P^* \ll P^*$. The isolation valve was then opened to allow the diffusion and flow through the carbon particle to occur. The total flux through the particle and the pressure difference across the particle were measured. Once the steady state has been achieved, the total permeability is calculated from

$$B_{\text{T}} = \frac{J_{\text{SS}}}{\Delta P/L} \tag{45}$$

Once this is done for one level of pressure P^*, the system pressure was brought to equilibrium at another pressure, and then the same procedure was repeated until the permeability curve versus loading can be generated. The steady state flux J_{SS} in Eq. (45) was determined from the measurement of the downstream reservoir versus time. Carrying out the mass balance around the downstream reservoir, we get

$$J_{\text{SS}} = B_{\text{T}} \frac{P_1 - P_2}{L} = \frac{V}{ART} \frac{\text{d}P_2}{\text{d}t} \tag{46}$$

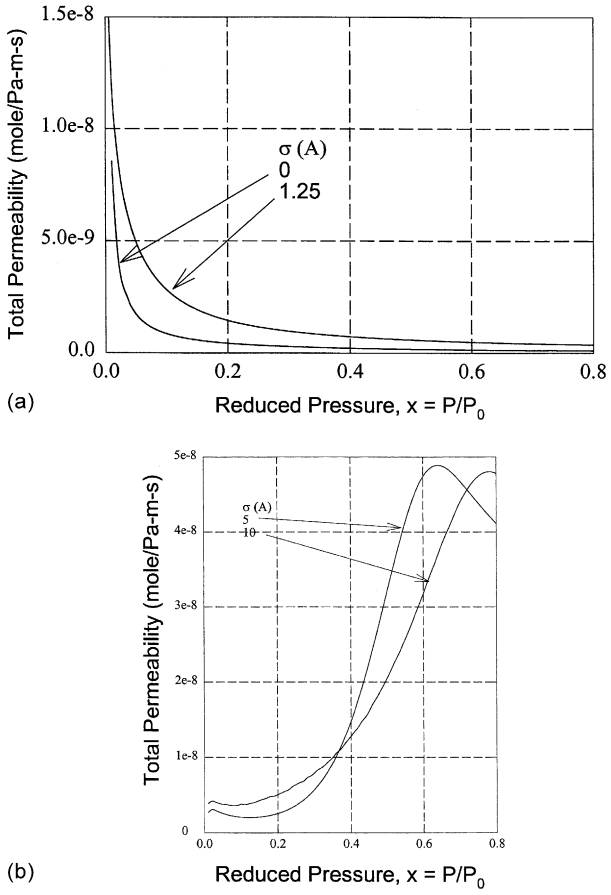

Fig. 6. Effect of variance on the permeability as a function of pressure.

where V is the volume of the downstream reservoir, A the cross-sectional area of the porous medium, and R the gas constant. Solving this equation subject to $t = 0$, $P_2 = P^*$, we get

$$\ln\left(\frac{P_1 - P_0^*}{P_1 - P_2(t)}\right) = \left(\frac{ARTB_T}{VL}\right)t \tag{47}$$

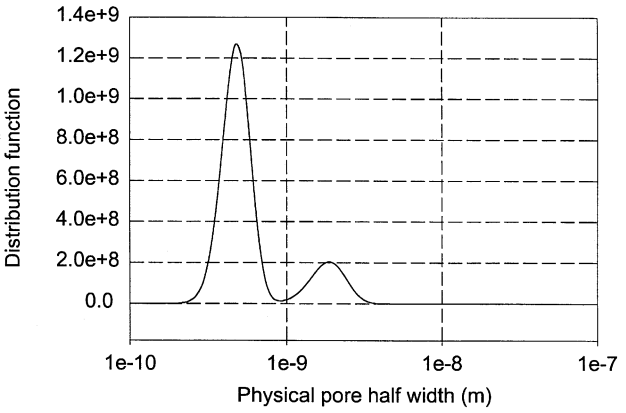

Fig. 7. Pore size distribution of Ajax activated carbon.

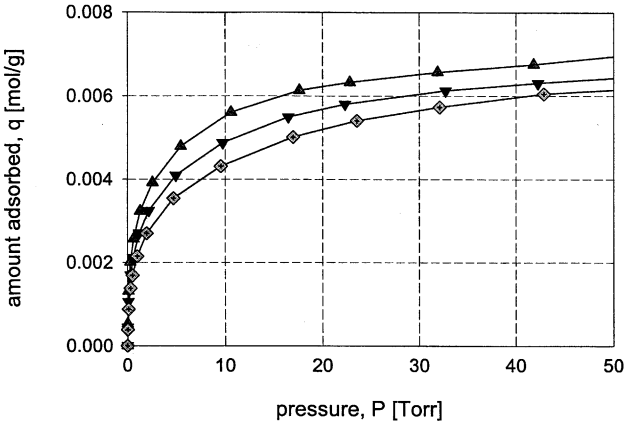

Fig. 8. Adsorption isotherm of benzene on Ajax activated carbon at 313, 323 and 333 K.

Thus a plot of $\ln[(P_1 - P_0^*)/(P_1 - P_2)]$ versus time will yield a straight line passing through the origin with a slope of $(ARTB_T/VL)$ from which the total permeability can be calculated.

Adsorption isotherms of benzene were obtained from the high accuracy volumetric apparatus. The results are shown in Fig. 8. Using the theory presented in this paper, we calculate the total permeability of benzene as a function of pressure as shown in Fig. 9. The only parameter we need for such simulation is the BET constant for benzene for a flat surface, which was found independently in our laboratory as 100. The experimental data are also shown in Fig. 9 as symbols. We see that the prediction, although does not match the data perfectly, is very good in the light of the prediction based on first principles as well as on fundamental parameters, such as particle characteristics, like PSD, porosity, and adsorbate properties, such as viscosity, collision diameter, and interaction energy. The values of these parameters used

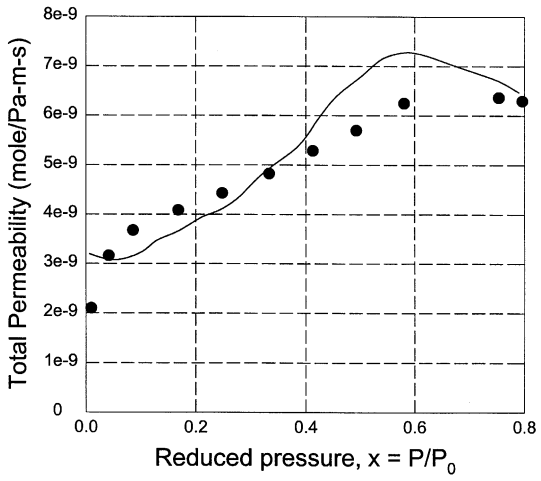

Fig. 9. Prediction of the benzene permeability versus experimental data.

in the simulation of Fig. 9 are given below:

Collision diameter of benzene	$\sigma_{ff} = 3.5 \times 10^{-10}$ m
Collision diameter of carbon	$\sigma_{ss} = 3.4 \times 10^{-10}$ m
BET C constant for benzene for flat surface	$C_{BET} = 100$
Heat of adsorption for benzene for flat surface	$Q = 30$ kJ/mol
Viscosity of liquid benzene at 303 K	7×10^{-4} Pa s
Viscosity of benzene vapor at 303 K	8×10^{-6} Pa s
Surface tension of benzene at 303 K	0.03 N/m
Liquid molar volume of benzene	8×10^{-5} m^3/mol
Vapor pressure of benzene at 303 K	16 kPa
Total porosity of activated carbon	0.71
Surface diffusivity	1×10^{-11} m^2/s

4. Conclusions

We have presented a detailed theoretical study of diffusion and flow of sub-critical fluids in activated carbon. The permeability is found to be dominated by pores having size less than 20 A or greater than 4000 A. The former is by flow of condensate, while the latter is by Knudsen diffusion and gaseous viscous flow. The theory was tested with flow of benzene through a commercial activated carbon, and the agreement was found to be very good, in the light that there are no fitting parameter in the model.

Acknowledgements

Supports from the Australian Research Council is gracefully acknowledged.

References

[1] F.B. Aarden, P.J.A.M. Kerkhof, A.J.J. van der Zanden, Capillary transport in adsorption from liquid phase on activated carbon, AIChE J. 45 (1999) 268–275.
[2] B. Abeles, L.F. Chen, J.W. Johnson, J.M. Drake, Capillary condensation and surface flow in microporous Vycor glass, Israel J. Chem. 31 (1991) 99–106.
[3] R.M. Barrer, Two phase flow of adsorbed vapours, Can. J. Chem. 41 (1963) 1768–1781.
[4] S. Brunauer, P.H. Emmett, E. Teller, Adsorption of gases in multiplayer layers, J. Am. Chem. Soc. 60 (1938) 309–319.
[5] P.C. Carman, F.A. Raal, Diffusion and flow of gases and vapours through micropores. III. Surface diffusion coefficients and activation energies, Proc. R. Soc. London A 209 (1951) 38–58.
[6] P.C. Carman, F.A. Raal, Diffusion and flow of gases and vapours through micropores. IV. Flow of capillary condensate, Proc. R. Soc. London A 211 (1952) 526–535.
[7] P.C. Carman, Properties of capillary-held liquids, J. Phys. Chem. 57 (1953) 56–64.
[8] Y.D. Chen, R.T. Yang, Surface diffusion of multilayer adsorbed species, AIChE J. 39 (1993) 599–606.
[9] Y.D. Chen, R.T. Yang, Surface and mesoporous diffusion with multiplayer adsorption, Carbon 36 (1998) 1525–1537.
[10] Y.D. Chen, R.T. Yang, Concentration dependence of surface diffusion and zeolitic diffusion, AIChE J. 37 (1991) 1579–1582.
[11] L.S. Darken, Diffusion, mobility and their interrelation through free energy in binary metallic systems, Trans. AIME 175 (1948) 184–201.
[12] P. Debye, R.L. Cleland, Flow of liquid hydrocarbons in porous Vycor, J. Appl. Phys. 30 (1959) 843–849.
[13] D.D. Do, A model for surface diffusion of ethane and propane in activated carbon, Chem. Eng. Sci. 51 (1996) 4145–4158.
[14] P.E. Eberly Jr., D.B. Vohsberg, Diffusion of benzene and inert gases through porous media at elevated temperatures and pressures, Trans. Faraday Soc. 61 (1965) 2724–2735.
[15] D.H. Everett, J.C. Powl, Adsorption in slit-like and cylindrical micropores in the Henry's law region, J. Chem. Soc., Faraday Trans. 72 (1976) 619–636.
[16] E.A. Flood, R.H. Tomlinson, A.E. Leger, The flow of fluids through activated carbon rods. Part I, Can. J. Chem. 30 (1952) 349–371.
[17] E.A. Flood, R.H. Tomlinson, A.E. Leger, The flow of fluids through activated carbon rods. Part II. The pore structure of activated carbon, Can. J. Chem. 30 (1952) 372–385.
[18] E.A. Flood, R.H. Tomlinson, A.E. Leger, The flow of fluids through activated carbon rods. Part III. The flow of adsorbed fluids, Can. J. Chem. 30 (1952) 389–410.
[19] E.R. Gilliland, R.F. Baddour, J.L. Russell, Rates of flow through microporous solids, AIChE J. 4 (1958) 90–96.
[20] J.M. Haynes, R.J.L. Miller, Surface diffusion and viscous flow during capillary condensation, in: J. Rouquerol, K.S.W. Sing (Eds.), Adsorption at the Gas–Solid and Liquid–Solid Interface, Elsevier, Amsterdam, 1982, pp. 439–447.
[21] K. Higashi, H. Ito, J. Oishi, Surface diffusion phenomena in gaseous diffusion. I. Surface diffusion of pure gas, J. Atomic Energy Soc. Jpn. 5 (1963) 846–853.
[22] W.B. Innes, Use of a parallel plate model in calculation of pore size distribution, Anal. Chem. 29 (1957) 1069–1073.
[23] W. Jost, Diffusion in solids, liquids and gases, Academic Press, New York, 1952.
[24] M.E. Kainourgiakis, A.K. Stubos, N.D. Konstantinou, N.K. Kanellopoulos, V. Milisic, A network model for the permeability of condensable vapors through mesoporous media, J. Memb. Sci. 114 (1996) 215–225.
[25] A. Kapoor, R.T. Yang, Surface diffusion on energetically heterogeneous surfaces — an effective medium approximation approach, Chem. Eng. Sci. 45 (1990) 3261–3270.
[26] A. Kapoor, R.T. Yang, Surface diffusion on energetically heterogeneous surfaces, AIChE J. 35 (1989) 1735–1738.
[27] E.S. Kikkinides, K.P. Tzevelekos, A.K. Stubos, M.E. Kainourgiakis, N.K. Kanellopoulos, Application of effective medium approximation for the determination of the permeability of condensable vapors through mesoporous media, Chem. Eng. Sci. 52 (1997) 2837–2844.
[28] K.H. Lee, S.T. Hwang, The transport of condensable vapours through a microporous Vycor glass membrane, J. Colloid Interf. Sci. 110 (1986) 544–555.
[29] H. Marsh, Introduction to Carbon Science, Butterworths, London, 1989.
[30] C. Nguyen, D.D. Do, A new method for the characterisation of porous materials, Langmuir 15 (1999) 3608–3615.
[31] D. Nicholson, P. Petropoulos, Calculation of the surface flow of a dilute gas in model pore from first principles. Part III. Molecular gas flow in single pores and simple model porous media, J. Colloid Interf. Sci. 106 (1985) 538–546.
[32] M. Okazaki, H. Tamon, R. Toei, Interpretation of surface flow phenomenon of adsorbed gases by hopping model, AIChE J. 27 (1981) 262–270.
[33] M. Okazaki, Roles of capillary condensation in adsorption, in: M. Suzuki (Ed.), Fundamentals of Adsorption, 1992, pp. 13–26.
[34] G.K. Papadopoulos, J.H. Petropoulos, Experimental verification of a proposed unified formulation of adsorbate transport in mesoporous media over the full vapour pressure range, J. Chem. Soc., Faraday Trans. 92 (1996) 3217–3223.

[35] J.H. Petropolous, G.K. Papadopoulos, Unified formulation of isothermal adsorbate flow in mesoporous media over the full vapor pressure range, J. Memb. Sci. 101 (1995) 127–133.
[36] J.H. Petropoulos, Model evaluation of adsorbate transport in mesoporous media in the multiplayer adsorption region, Langmuir 12 (1996) 4814–4816.
[37] I. Prasetyo, D.D. Do, Adsorption kinetics of light paraffins in AC by a constant molar flow-rate method, AIChE J. 45 (1999) 1892–1900.
[38] P. Rajniak, R.T. Yang, Unified network model for diffusion of condensable vapours in porous media, AIChE J. 42 (1996) 319–331.
[39] H. Rhim, S.T. Hwang, Transport of capillary condensate, J. Colloid Interf. Sci. 52 (1975) 174–181.
[40] H. Tamon, M. Okazaki, R. Toei, Flow mechanism of adsorbate through porous media in presence of capillary condensation, AIChE J. 27 (1981) 271–277.
[41] H. Tsujikawa, T. Osawa, H. Inoue, Separation of benzene and nitrogen by permeation through porous Vycor glass, Int. Chem. Eng. 27 (1987) 479–487.
[42] K.P. Tzevelekos, E.S. Kikkinides, A.K. Stubos, M.E. Kainourgiakis, N.K. Kanellopoulos, On the possibility of characterising mesoporous materials by permeability measurements of condensable vapours: theory and experiments, Adv. Colloid Interf. Sci. 76 (1998) 373–388.
[43] K.P. Tzevelekos, G.E. Romanos, E.S. Kikkinides, N.K. Kanellopoulos, V. Kaselouri, Experimental investigation on separations of condensable from non-condensable vapors using mesoporous membranes, Microporous Mesoporous Mater. 31 (1999) 151–162.
[44] R.J.R. Uhlhorn, K. Keizer, A.J. Burggraaf, Gas transport and separation with ceramic membranes. Part I. Multilayer diffusion and capillary condensation, J. Memb. Sci. 66 (1992) 259–269.
[45] A.J.J. van der Zanden, W.J. Coumans, P.J.A.M. Kerkhof, A.M.E. Schoenmakers, Isothermal moisture transport in partially saturated porous media, Drying Technol. 14 (1996) 1525–1542.
[46] R.T. Yang, J.B. Fenn, G.L. Haller, Modification to the Higashi model for surface diffusion, AIChE J. 19 (1973) 1052–1053.